

Characteristics of ZnO-based semiconductor ceramics doped with GeO₂ and PbO

Osama A. Desouky¹, Mostafa M. H. Khalil²

¹ Bilbis Higher Institute of Engineering (BHIE), Bilbis, Sharqia, Egypt

² Chemistry Department, Faculty of Science, Ain Shams University, 11566, Abbassia, Cairo, Egypt

Abstract: *The effect of GeO₂ and PbO on physical, microstructure, and the electrical properties of ZnO based ceramics is investigated. A decrease in water absorption was recorded with rise in maturing temperature and increase in time of soaking. A minimum water absorption was displayed in specimens fired at 1000 °C for 2 hours. The average grain size decreases initially as GeO₂ content increases up to 2 mol %. The grain size of ZnO decreases greatly, as the Ge-rich phase inhibits grain growth ZnO decreases. The decrease of capacitance in (pf), dielectric constant (ϵ') and consequently increase (AC) conductivity with increasing frequency (1 – 20) KHz was investigated.*

1. Introduction

Metal oxides play a very important role in many areas of chemistry, physics and materials science [1 –6]. Lead exists in three oxidation states: Pb(0), the metal; Pb(II); and Pb(IV). Lead monoxide is the most important commercial compound of lead. Litharge is used primarily in the manufacture of various ceramics products. Because of its electrical and electronic properties, litharge is also used in capacitors, Videocon tubes, and electro photographic plates, as well as in ferromagnetic and ferroelectric materials [7]. The outer electronic structure of germanium is the same as silicon, but its atomic radius is greater. This suggests a weaker bonding between germanium and oxygen which leads to better transmission than silicon. Germinates and GeO₂ containing glasses have become important materials in the telecommunications and optics industries. Among these glasses, lead germinate are interest because of several characteristics that make them promising materials for applications as new lasing materials and up converters. The metal elements are able to form a large diversity of oxide compounds [8]. These can adopt a vast number of structural geometries with an electronic structure that can exhibit metallic, semiconductor or insulator character. In technological applications, oxides are used in the fabrication of microelectronic circuits, sensors, piezoelectric devices, fuel cells, coatings for the passivation of surfaces against corrosion, and as catalysts. In the emerging field of nanotechnology, a goal is to make nanostructures or nano arrays with special properties with respect to those of bulk or single particle species.[9-13]. Zinc oxide (ZnO), a wide band gap (3.4 eV) II-VI compound semiconductor, has a stable Wurtzite structure with lattice spacing $a = 0.325$ nm and $c = 0.521$ nm. It has attracted intensive research effort for its unique properties and versatile applications in transparent electronics, ultraviolet (UV) light emitters, piezoelectric devices, chemical sensors and spin electronics [14-23]. Doping of Ge, which is one of the group IV atoms, into zinc oxide is expected to be harmless to the use of the oxide in devices including a-Si layer. There is, however, only one report on the Ge-doped zinc oxide films. Sato et al.[24] investigated the Ge-doped zinc oxide thin films prepared by an RF sputtering system with an external solenoid coil and reported that the lowest resistivity of $7.4 \times 10^{-4} \Omega \text{cm}$ was

obtained using a sputtering target including (2 mass% of Ge) but the true concentration of impurity in the deposited film was not shown. Impurity doped zinc oxide films show a maximum of conductivity at a proper dopant concentration, namely excess of impurity doping causes deterioration in the electrical property. With a view to improve the electrical property of impurity doped zinc oxide films, it is required to understand the relationship between various properties of the films and the true concentration of doped impurities. The doping of Ge caused reduction of resistivity of the films. At about 3% of Ge content the minimum resistivity of about $2 \times 10^{-3} \Omega \text{cm}$ was obtained. The improvement of conductivity would be attributed to an increase in the carrier concentration by the Ge doping. With high content of Ge, however, the crystalline structure changed and the resistivity of the film increased [25,26]. Zinc oxide varistors are semiconductor ceramic devices manufactured by sintering devices, which are widely used for voltage stabilization and transient surge suppression in electric power systems and electronic circuits. These ceramic devices exhibit high non-linear current-voltage characteristics, and each region of the I-V curve plays an important part in voltage stabilization and transient surge suppression [27]. The electrical performance of ZnO varistors critically depends on the nano- micro-, and macro-structural characteristics. In this work , the effects of GeO₂ and PbO content on water absorption ,total shrinkage, the microstructure and the electrical characteristics of the ZnO-ceramics .The samples were examined by X-ray powder diffraction (XRD), scanning electron microscopy (SEM) and standard electrical measurement procedures were used.

2. Materials and Methods

Reagent grade (99.5%) powders of ZnO, GeO₂ and PbO were used as starting materials. Compositions of ZnO ceramic semiconductors were summarized in Table 1. Batches were abbreviated as A1, A2, A3, A4, A5, A6, A7 and A8. Discs with 1.2 cm diameter and 0.2 cm thickness were used. These discs were processed by a semi-dry press method under 70 KN. The specimens were subjected to thermal treatment to select the proper maturing temperature for each mix. Three discs were always fired in muffle kiln with a rate of heating of 5 °C/ min in the temperature range

between (800 -1000) °C for 2 hours. The sinter ability of the different samples was determined in terms of physical properties. The optimum firing temperature for each mix was deduced from the determination of the following parameters; firing shrinkage, apparent porosity, bulk density and water absorption. The method given is according to the ASTM standard (C71, C72) [28]. The starting materials namely; ZnO, GeO₂ and PbO were examined by XRD. Using Philips apparatus type 170, a vanadium ($\lambda=1.54 \text{ \AA}$) and Ni-filter. In Metallurgy Research Center, Egypt. A continuous plot of intensity for 2θ values from 4 to 80 was made at a scanning speed of 1°/ minute, with a paper speed of 10 mm/min. The apparent sintered samples were lapped (1mm thick) and then polished. To measure the electrical properties, silver pastes were coated on both sides of the sintered samples. The PM 6304 programmable automatic RCL meter was used for precise measurements of resistance, capacitance and inductance. The capacitance and resistance at constant temperature were measured at different between (1-30) KHz, the respective permittivity [ϵ], resistivity and conductivity were calculated. The microstructures of samples were examined via the scanning electron microscopy (SEM, Joel-JEM. T 200).

3. Results and Discussions

Results of water absorption of different mixes are shown in Fig. 1. A decrease in water absorption was recorded with rise in maturing temperature and increase in time of firing. Minimum water absorption was displayed in specimens fired at 1000 °C for 2 hours. The ratio of bulk density at the selected maturing temperature with respect to the true density is a measure for the degree of densification reached. Usually a percent not exceeding 93% was displayed by different mixes. From the above mentioned results, it is evident that better densification and less water absorption are achieved in all mixes fired at 1000 °C for 2 hour. Therefore, this temperature was selected as the proper maturing temperature for all mixes. Minimum water absorption of 2% was achieved by mix (A₅) which containing ZnO and 2.6955 mol% PbO. The result of firing shrinkage showed an increase with rise in temperature and in time of soaking as shown in Fig .2. Maximum shrinkage values were attained in mixes fired at 1000 °C for 2 hours. The mixes showed an increase in firing shrinkage with increase in GeO₂ and PbO added, a maximum of %31.5789 was displayed in mix A₁, A₂ which containing ZnO and 1.281 mol% , 2.555 mol % GeO₂, respectively and in mix A₄, A₆ which containing ZnO and 1.3593mol% , 4.3004 mol% PbO respectively. From the results, PbO and GeO₂ improved densification by minimizing the percent of closed pores. Mix (A₅) shows max densification. Lenel [29], German [30], and Osama et al [31] studied sintering of ZnO grain in the system ZnO-Bi₂O₃ and ZnO-Ti₂O₃ and reported that better densification was achieved in the presence of liquid phase. According to the binary system ZnO-Bi₂O₃, a eutectic reaction occurs at 740 °C, resulting in the presence of ZnO-4Bi₂O₃ and ZnO which is of low density.

Table 1: Composition of different mixes in mol%

Oxides		ZnO mol%	PbO mol%	GeO ₂ mol%
Group(V)	A1	99	-	1
	A2	98	-	2
	A3	97	-	3
	A4	99.5	0.5	-
	A5	99	1	-
	A6	98	2	-
	A7	99	0.5	0.5
	A8	99	1	1

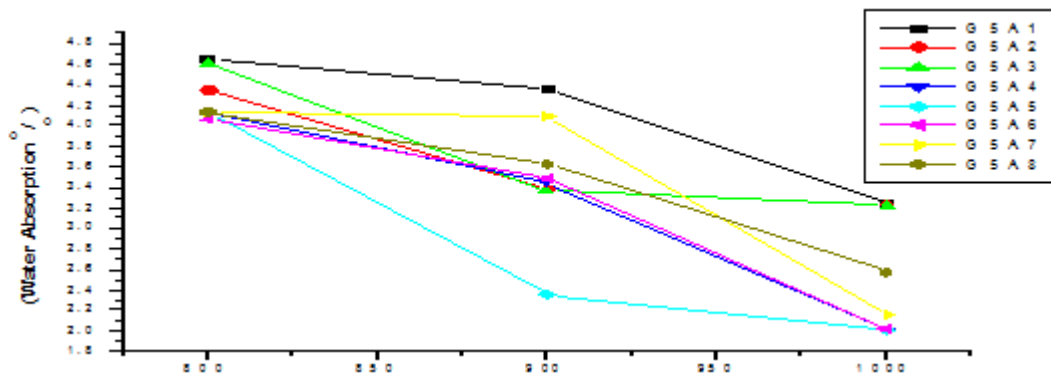


Figure 1: Water absorption % of different mixes at different temperatures for 2 hours.

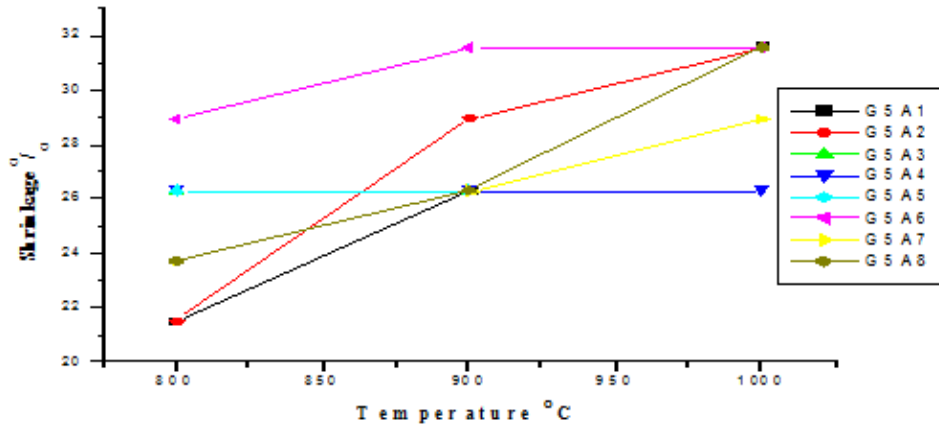


Figure 2: Shrinkage% of different mixes at different temperature for 2 hours

X - ray diffraction analyses of sintered samples reveal no formation of new phases, but lattice constants of phases were changed after sintering. Lattice constants of each sample were changed in different extents depending on the phases affinity to a particular ion and on overall semiconductor composition. Fig.3. shows the X-ray diffraction pattern of sample (A₅) annealed at 1000 °C for 3 hour in oxygen atmosphere in which zinc oxide – ZnO, Hexagonal phase – a 3.2488 – b 3.2488 – c 5.2054 at about 2θ = 31.843 d = 2.80800Å, 2θ = 34.518 d = 2.59630Å, 2θ = 36.338 d = 2.47036Å, 2θ = 47.608 d = 1.90853Å, 2θ = 56.655 d = 1.62336Å, 2θ = 62.921 d = 1.47591 Å, 2θ = 67.989 d = 1.37771 Å, 2θ = 69.112 d = 1.35805 Å, 2θ = 76.968 d = 1.23783Å, lead oxide Massicot-PbO, orthorhombic phase – a 5.89310 – b 3.2488 – c 5.2054 at about 2θ = 32.625 d = 2.7425Å, 2θ = 59.404 d = 1.55464Å. Fig.3. shows the X-ray diffraction pattern of sample (A₈) annealed at 1000 °C

for 3 hour in oxygen atmosphere in which zinc oxide , ZnO (Hexagonal phase – a 3.2417 – b 3.2417 – c 4.9893 at about 2θ = 31.93 d = 2.8005A°, 2θ = 34.622 d = 2.58872A°, 2θ = 36.48 d = 2.46480A°, 2θ = 47.737 d = 1.90367A°, 2θ = 56.765d = 1.62048A°, 2θ = 63.062 d = 1.47296A°, 2θ = 68.137 d = 1.37508A°, 2θ = 69.251 d = 1.35566A°, 2θ = 72.772 d = 1.29850A°, 2θ = 77.109 d = 1.23592Å, lead oxide – PbO , orthorhombic phase – a 5.6085 – b 5.6036 – c 4.9893 at about 2θ = 13.93 d = 2.80059A°, 2θ = 36.422 d = 2.46480A°, lead oxide – PbO₂, Tetragonal phase – a 4.961 – b 4.96100 – c 3.38500 at about 2θ = 25.17 d = 3.53525A°, 2θ = 31.93 d = 2.80059A°, 2θ = 28.864 d = 3.09074A°, Germanium oxide , GeO₂ – Cubic phase – a 5.4100 - b 5.4100 - c 5.4100 at about 2θ = 28.864 d = 3.09074A°, 2θ = 33.453 d = 2.67648A°, 2θ = 47.737 d = 1.90367A°, 2θ = 77.109 d = 1.23592A°.

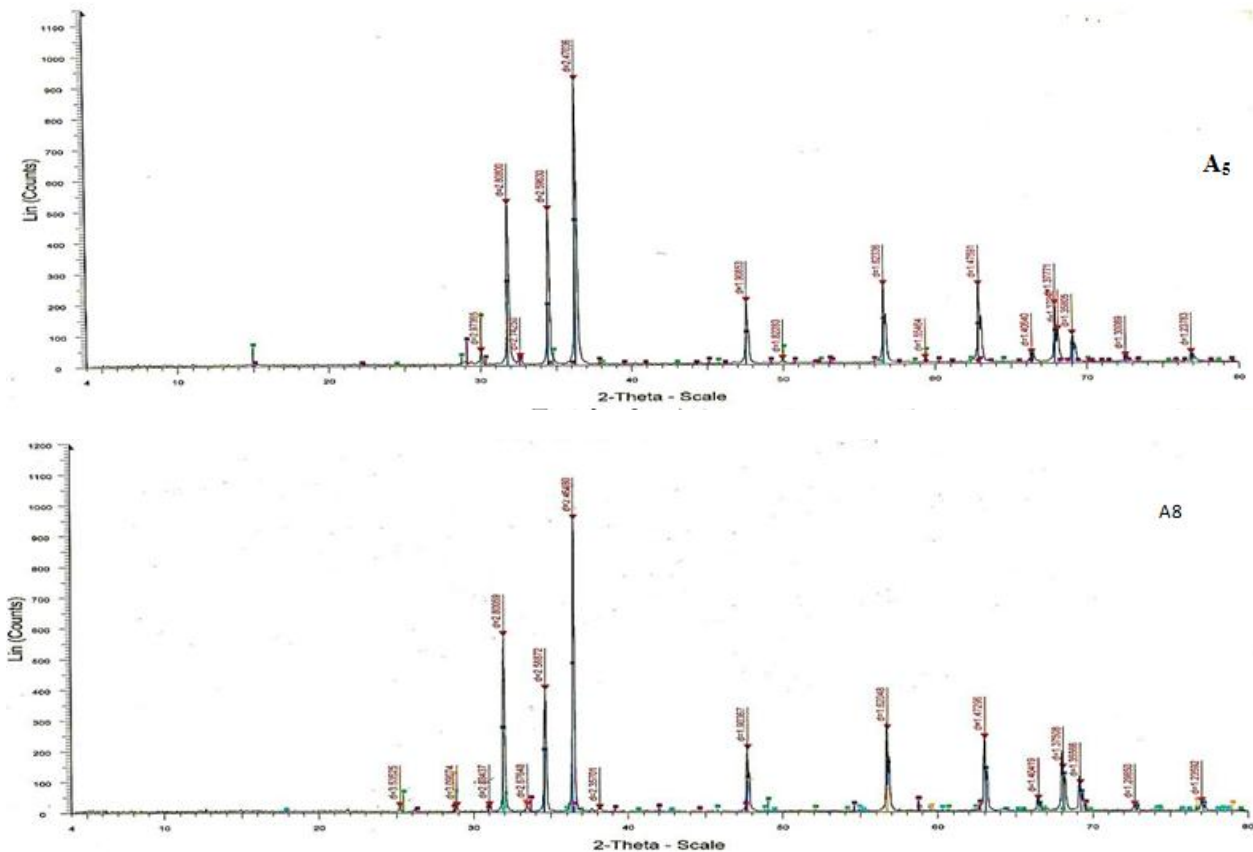


Figure 3: XRD of mixes A5 & A8 annealed at 1000 °C for 3 hour

The SEM can seen clearly from Figs (4 -7) the grain size of ZnO decreases greatly because Ge-rich phase inhibits grain growth ZnO decreases. SEM of mix (A₁), a more uniform grain size can be obtained when sintering at 1000 °C for 3 hour. The average grain size decrease initially as GeO₂ content increases up to 2 mol %.SEM of mix A₂ present in Fig.5. shows a homogeneous primary particle size of (0.1–1) μm, ZnO grains dissolution of GeO₂ between ZnO grains. The SEM of A₄, present in Fig.6., shows ZnO grain of various size (0.1 and 0.2μm). Submicron pores occur at triple points at the grain corners, which ZnO-ZnO grain functions are devoid of them.SEM of mix (A₇) present in Fig.7.Shows liquid phase in the triple points. Liquid phase and exsolution in the triple point and distribution concerted on the pores, a moreless uniform grain size.

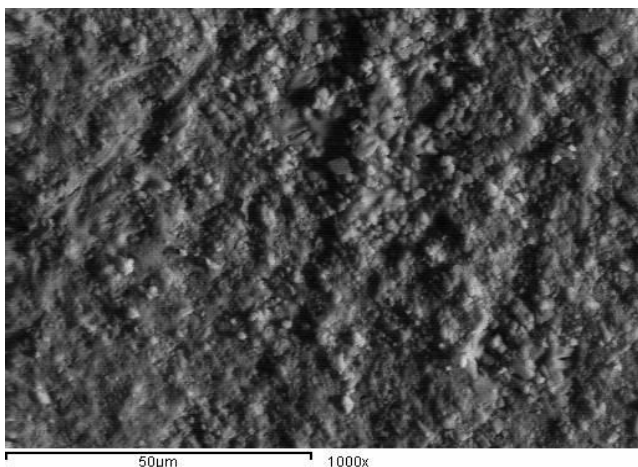


Figure 4: SEM of mix A₁, thermally etched, shows a more uniform grain size, X=1000

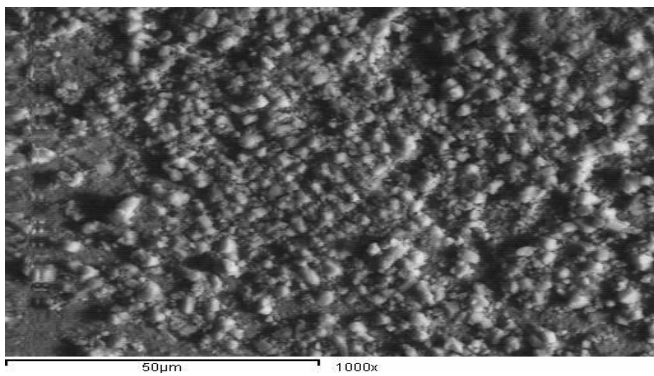


Figure 5: SEM of mix A₂, thermally etched surface, X = 1000

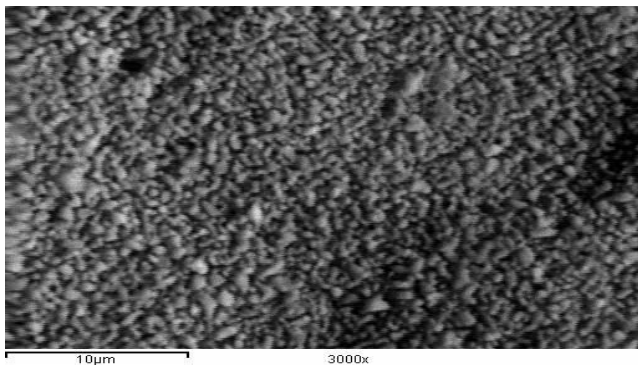


Figure 6: SEM of mix A₄, Thermally etched surface, general view X =3000

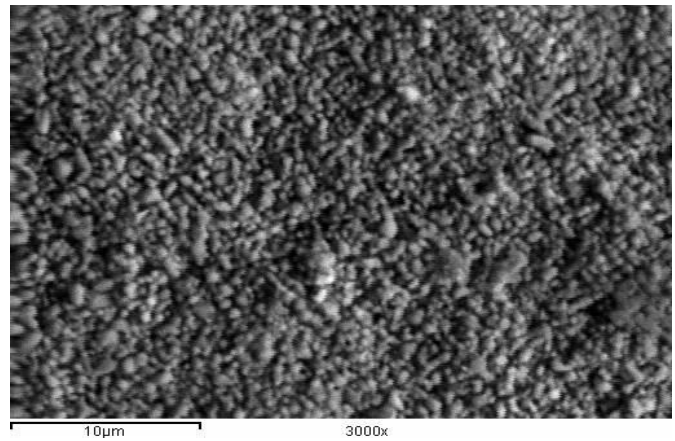


Figure 7: SEM of mix A₅,thermally etched surface showing contact surfaces between ZnO grains and present of exsolution of Ge - rich particles, X=3000.

For the samples namely A₁,A₂ and A₃, the increase of the mol% GeO₂ leading to increase the capacitance, the values of capacitance for sample A₁ ranged between (2.867-2.6703) , sample A₂ ranged between (3.1987-3.079) but for sample A₃ ranged between (13.1987-9.2143). Also for the samples , namely (A₄,A₅ and A₆) , the increase of mol% PbO leading to increase the capacitance .The values of capacitance for A₄,A₅ and A₆ ranged between (2.4742-2.3486), (10.473-8.191) and (11.108-10.312) respectively, while for the last sub group namely A₇ and A₈ have a low values in comparison with that of first and second subgroup (i.e. the presence of GeO₂ and PbO together leading to decrease of the capacitance of sample A₇ and A₈ which ranged between (9.3035-6.5199) and (7.5539-5.5578) respectively.Fig.8 shows the variation of dielectric constant (ϵ') with frequency (1-20)KHz , it is clearly observed from this Fig that the dielectric constant (ϵ') decreases with increasing frequency for different samples, in a behavior similar to that exhibited by most semiconducting materials for samples powder ZnGeO₃ namely A₁, A₂ and A₃, the increase of mol% GeO₂ leading to increase the dielectric constant (ϵ'), also the same behavior was observed in samples powder ZnPbO₂ namely A₄, A₅, and A₆ i.e the increase of mol% PbO leads to increase the values of dielectric constant with increasing frequency (1-20) KHz. While for samples ZnPbGeO₄ namely A₇and A₈ have a low values of dielectric constant (ϵ') in comparison with hat of ZnPbO₂ and ZnGeO₂ powders. i.e. the presence of GeO₂ and PbO to gather with ZnO leading to decrease of dielectric constant with increasing frequency (1-20) KHz. For samples A₁, A₄, and A₇, the dielectric constant (ϵ') are maintained at constant values as frequency increases up to 10 KHz, this attributed to dielectric relaxation. The relaxation is presumably due to change of polarization mode ZnGePbO₄, ZnGeO₂ and ZnPbO₂ powders with frequency, transferring from dipole polarization to ionic polarization reign. The electrical conduction mechanism can be explained by the electron hopping model of Heike's and Johnston [32]. Mansour reported that local displacements of electrons in the direction of the applied electric field, these displacement determine the polarization of the ferrite [33].It is know that the effect of polarization is to reduce the field inside the medium. Therefore, the dielectric constant of a substance may be decrease substantially as the frequency is increase. In general Figs. 8,9 show the decrease of capacitance in (pf) ,

dielectric constant (ϵ') and consequently increase (AC) conductivity with increasing frequency (1 – 20) KHz. This behavior reflects the transition from one process to another process, which may be related to a thermally activated charged particle in accordance with Maxwell – Wagner mechanism [34, 35]. This results in a monotonous decrease in the value of dielectric constant on increasing frequency for all the concentration. This observation may be attributed to a combined contribution to the dielectric constant due to electric, ionic, interfacial polarization at low frequencies. At higher frequency, charge species present in the material become mobile and play a predominant role in the conduction process due to decrease in the resistive properties revealed by the resistivity spectrum results Figs. 8-10. This is because the ionic motion is sensitive to the alternating field variation at higher frequencies resulting in the release of space charge

present. This is due to the presence of space charge polarization [36]. The results of resistance and resistivity of different mixes with different additives are graphically represented as a function of frequency in Fig.10. The resistance and resistivity values are higher at room temperature in the low frequency. A decrease in resistance and resistivity with rise in frequencies indicates a possibility of increase in the AC conductivity with increased frequency. The merger of real part of resistivity in the higher frequency domain suggests release of space charge and a consequent lowering of the barrier properties in the materials. The valence of added oxides has larger influence on the capacitance, resistance, dielectric constant, resistivity and conductivity values of fabricated semiconductors.

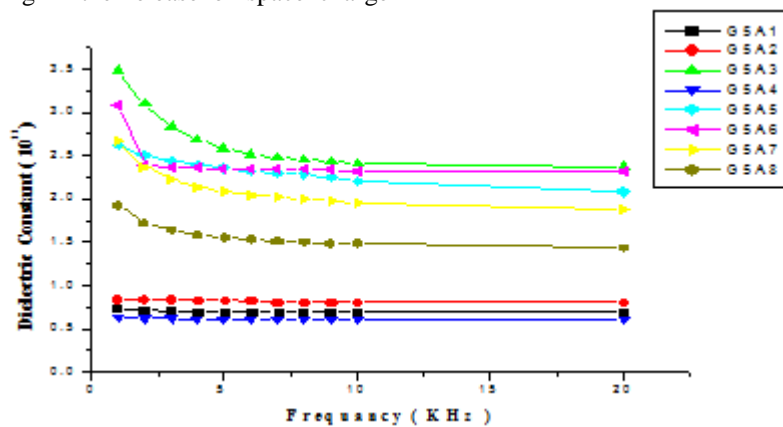


Figure 8: Effect of frequency (KHz) on dielectric constant of different mixes

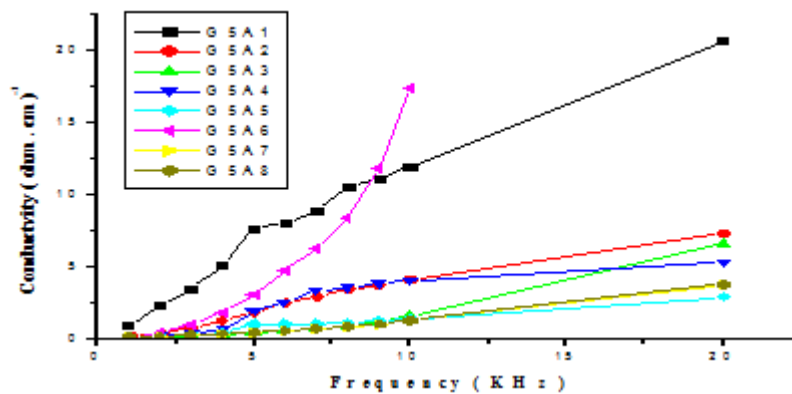


Figure 9: AC Conductivity as a function of frequency for mixes of different mixes

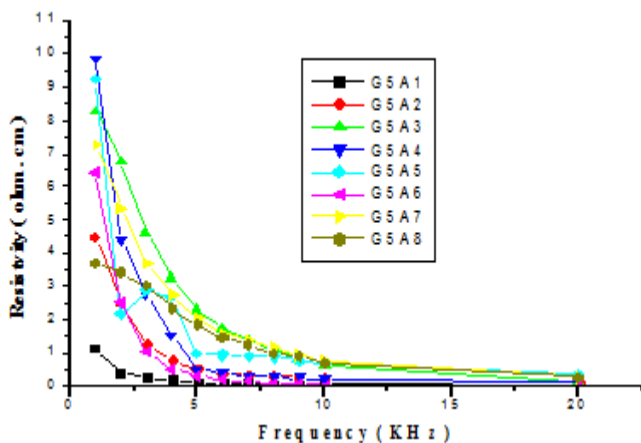


Figure 10: Effect of Frequency (KHz) on Resistivity ($\Omega \cdot \text{cm}$) different mixes.

4. Conclusions

In polycrystalline semiconductors, the trapping of charge at the grain boundaries has a decisive influence on the electrical transport properties by means of the formation of electrostatic potential barriers. Minimum water absorption was displayed in specimens fired at 1000 °C for 2 hours. The better densification and less water absorption are achieved in all mixes fired at 1000 °C for 2 hour. Therefore, this temperature was selected as the proper maturing temperature for all mixes. The mixes showed an increase in firing shrinkage with increase in GeO_2 and PbO added, a maximum of % 31.5789 was displayed in mixes A_1 , A_2 . The SEM of mix A_3 , shows the distribution of GeO_2 in the intergranular region, a more less uniform grain size. SEM of mix (A_7) shows liquid phase in the triple points. Liquid

phase and exsolution in the triple point and distribution concerted on the pores. The dielectric constant decrease with increasing frequency for different samples, in a behavior similar to that exhibited by most semiconducting materials for samples powder ZnGeO₃. The increase of mol% PbO leads to increase the values of dielectric constant with increasing frequency (1-20) KHz. The presence of GeO₂ and PbO together with ZnO leading to decrease of dielectric constant with increasing frequency (1-20) KHz.. This observation may be attributed to a combined contribution to the dielectric constant due to electric, ionic, interfacial polarization at low frequencies. At higher frequency, charge species present in the material become mobile and play a predominant role in the conduction process due to decrease in the resistive properties revealed by the resistivity spectrum results. This is due to the presence of space charge polarization.

References

- [1] Noguera, C. *Physics and Chemistry at Oxide Surfaces*; Cambridge University Press: Cambridge, UK, 1996.
- [2] Kung, H.H. *Transition Metal Oxides: Surface Chemistry and Catalysis*; Elsevier: Amsterdam, 1989.
- [3] Henrich, V.E.; Cox, P.A. *The Surface Chemistry of Metal Oxides*; Cambridge University Press: Cambridge, UK, 1994.
- [4] Wells, A.F. *Structural Inorganic Chemistry*, 6th ed; Oxford University Press: New York, 1987.
- [5] Rodríguez, J.A., Fernández-García, M; (Eds.) *Synthesis, Properties and Applications of Oxide Nanoparticles*. Wiley: New Jersey, 2007.
- [6] Fernández-García, M.; Martínez-Arias, A.; Hanson, J.C.; Rodríguez, J.A. *Chem. Rev.* 104(2004) 4063.
- [7] E.J. Ritchie, *Lead Oxides*, Independent Battery Manufacturers Association, Inc., Largo, FL.(1974).
- [8] Wyckoff, R.W.G. *Crystal Structures*, 2nd ed; Wiley: New York, 1964.
- [9] Gleiter, H. *Nanostruct. Mater.* 6 (1995) 3.
- [10] Valden, M.; Lai, X.; Goodman, D.W. *Science*, 281 (1998) 1647.
- [11] Rodriguez, J.A.; Liu, G.; Jirsak, T.; Hrbek, Chang, Z.; Dvorak, J.; Maiti, A. *J. Am. Chem. Soc.* 124 (2002) 5247.
- [12] Baumer, M.; Freund, H.-J. *Progress in Surf. Sci.* 61(1999) 127.
- [13] Trudeau, M.L.; Ying, J.Y. *Nanostruct. Mater.* 7 (1996) 245.
- [14] K. Nomura, H. Ohta, K. Ueda, T. Kamiya, M. Hirano, and H. Hosono, *Science*.300(2003)1269.
- [15] T. Nakada, Y. Hirabayashi, T. Tokado, D. Ohmori, and T. Mise, *Sol. Energy*.77 (2004) 739.
- [16] S. Y. Lee, E. S. Shim, H. S. Kang, S. S. Pang, and J. S. Kang, *Thin Solid Films* 31 (2005) 437.
- [17] R. Könenkamp, R. C. Word, and C. Schlegel, *Appl. Phys. Lett.* 85(2004) 6004 .
- [18] S. T. Mckinsty, and P. Muralt, *J. Electroceram.* 7 (2004) 12 .
- [19] Z. L. Wang, X. Y. Kong, Y. Ding, P. Gao, W. L. Hughes, R. Yang, and Y. Zhang, *Adv. Funct. Mater.* 14 (2004) 943 .
- [20] M. S. Wagh, L. A. Patil, T. Seth, and D. P. Amalnerkar, *Mater. Chem. Phys.* 84 (2004) 228 .
- [21] Y. Ushio, M. Miyayama, and H. Yanagida, *Sensor Actuat. B* 17 (1994) 221 .
- [22] H. Harima, *J. Phys.: Condens. Matter* 16 (2004) S5653 .
- [23] S. J. Pearton, W. H. Heo, M. Ivill, D. P. Norton, and T. Steiner, *Semicond. Sci. Technol.* 19(2004) R59.
- [24] H. Sato, T. Minami and S. Takata: *J. Vac. Sci. Technol. A* 11 (1993)2975.
- [25] M. Arita, M. Yamaguchi and M. Masuda *Materials Transactions* 45 (2004) 3180.
- [26] E.Mansour, G.El Damrawi ,R.E.Feton and H.Doweidar, *Eur. Phys.J. B.* 83 (2011) 133 .
- [27] Gupta TK. *J Am Ceram Soc.* 7 (1990) 1817.
- [28] Annual book of ASTM standards, ASTM standards on ceramics, American society for testing and material, 1966 .
- [29] Lenal, F.V, *Trans.,AIME*,175(1948)975 .
- [30] German,R.M., Plenum press, *Liquid phase sintering*, New York 1985.
- [31] Osama.A.Desouky, Saber E.Mansour, Ibrahim A. Ibrahim, El- Sayed. M. Nagim and Muhammad.I.Saleh.,*World Jorunal of Chemistry* 5 (2010)17.
- [32] R.R.Heikes and D.Johnston, *J.Chem.Phys.* 26(1957) 582 .
- [33] S. F. Mansour, *Egypt. J. Solids*,28 (2005) 263. .
- [34] k. s. lee, J, *phys. chem. solid* 57 (1996)333
- [35] E. Ortiz, R. A. Vargas, B. E. Mellander, *J. phys. chem. solids* 59 (1998)305 .
- [36] F. Shimizu, M. Takashige, S. Sawada,T. Yamaguchi, *J.phys.soc. Jpn.*62(1993) , 2964